

OSCILLATING RADIAL FLOW BETWEEN PARALLEL PLATES

A. F. ELKOUH

Mech. Eng. Dept.
Marquette Univ., Milwaukee, Wisconsin, U.S.A.

Abstract

An analysis is presented for laminar radial flow due to an oscillating source between parallel plates. The source strength varies according to $Q = Q_0 \cos \omega t$, and the solution is in the form of an infinite series in terms of a reduced Reynolds number, $R_a^* = Q_0/4\pi\nu a/(r/a)^2$. (Q_0 = amplitude of source strength, ω = frequency, a = half distance between plates, r = radial coordinate, t = time, and ν = kinematic viscosity.) The results are valid for small values of R_a^* and all values of the frequency Reynolds number, $\alpha = \omega a^2/\nu$. The effects of the parameters R_a^* and α are discussed.

Nomenclature

a	half distance between plates
\bar{r}	radial coordinate
r	dimensionless radial coordinate, \bar{r}/a
\bar{z}	axial coordinate
z	dimensionless axial coordinate, \bar{z}/a
\bar{t}	time
t	dimensionless time, $\bar{t}\nu/a^2$
R	dimensionless radial coordinate of a cross-section in the flow
\bar{u}	velocity component in radial direction
u	dimensionless velocity component in radial direction, $\bar{u}a/\nu$
\bar{v}	velocity component in axial direction
v	dimensionless velocity component in axial direction, $\bar{v}a/\nu$
\bar{p}	pressure
p	dimensionless pressure, $\bar{p}a^2/\rho\nu^2$
Q	instantaneous source strength
Q_0	amplitude of source strength
ω	frequency
R_a	amplitude of source Reynolds number, $Q_0/4\pi\nu a$
R_a^*	amplitude of reduced Reynolds number, R_a/r^2
α	frequency Reynolds number, $\omega a^2/\nu$

ρ	density
μ	viscosity
ν	kinematic viscosity, μ/ρ
$\bar{\tau}_1$	shear stress at the upper boundary
τ_1	dimensionless shear stress at the upper boundary, $\bar{\tau}_1/(\mu Q_0/4\pi a^2 \bar{r})$

§ 1. Introduction

Oscillating flow is of practical significance in many areas of engineering, e.g. acoustics, biomedical engineering, and lubrication. Oscillating radial flow is of primary interest in the design of thrust bearings and radial diffusers.

A system that has received considerable attention is that of flow in circular tubes, e.g. Uchida [1]. The only analysis published on oscillating radial flow is by Na, Neilsen, and Grossman [2]. In their analysis, a small sinusoidal oscillation in the flow rate about a finite mean value was considered. Their solution is valid for very small frequencies and for large distance from the center.

In this paper an analysis is presented for a system in which the flow rate varies sinusoidally about a zero-mean value. The solution obtained for the oscillation of the fluid is in the form of an infinite series expansion in terms of a reduced Reynolds number, $R_a^* = (Q_0/4\pi\nu a)/(\bar{r}/a)^2$, which signifies the importance of convective inertia. Another dimensionless group $\alpha = \omega a^2/\nu$, a frequency Reynolds number, also appears in the solution and signifies the effect of local inertia.

The effects of the parameters R_a^* and α on the pressure, velocity, and shear stress are presented. The results presented herein provide an understanding of the effect of frequency on the characteristics of laminar radial flow between parallel plates over the whole range of frequencies from $0 \rightarrow \infty$.

§ 2. Basic equations and solutions

a) *Basic equations*

Consider the nonsteady axially symmetric flow of a Newtonian fluid with constant properties between parallel infinite disks, which lie in the planes $\bar{z} = -a$ and $\bar{z} = +a$, Fig. 1. The flow through the system shown in Fig. 1 is due to a source, at $\bar{r} = 0$, whose strength varies according to

$$Q = Q_0 \cos \omega \bar{t}$$

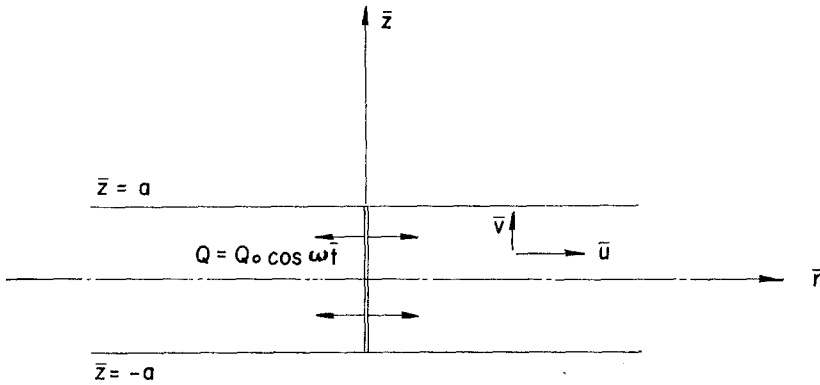


Fig. 1. Flow system and coordinates.

In terms of the dimensionless variables defined, see nomenclature, the Navier-Stokes equations are

$$\begin{aligned} \frac{\partial u}{\partial t} + u \frac{\partial u}{\partial r} + v \frac{\partial u}{\partial z} = \\ = - \frac{\partial p}{\partial r} + \left(\frac{\partial^2 u}{\partial r^2} + \frac{1}{r} \frac{\partial u}{\partial r} - \frac{u}{r^2} + \frac{\partial^2 u}{\partial z^2} \right) \end{aligned} \quad (1)$$

and

$$\frac{\partial v}{\partial t} + u \frac{\partial v}{\partial r} + v \frac{\partial v}{\partial z} = - \frac{\partial p}{\partial z} + \left(\frac{\partial^2 v}{\partial r^2} + \frac{1}{r} \frac{\partial v}{\partial r} + \frac{\partial^2 v}{\partial z^2} \right) \quad (2)$$

and the equation of continuity is

$$\frac{\partial u}{\partial r} + \frac{u}{r} + \frac{\partial v}{\partial z} = 0 \quad (3)$$

The boundary conditions for the flow system under consideration are

$$u = v = 0 \text{ at } z = \pm 1$$

and

$$\int_{-1}^{+1} u \, dz = \frac{2R_a}{r} \cos \alpha t \quad (4)$$

where $R_a = Q_0/4\pi\nu a$ is the amplitude of the source Reynolds number and $\alpha = \omega a^2/\nu$ is a dimensionless frequency parameter.

In order to obtain a solution for (1), (2) and (3), we assume the following expansions, which are valid for small values of R_a^* ($= R_a/r^2$), Elkouh [3]:

$$u = \frac{R_a}{r} \left\{ f'_0(z, t) + \left(\frac{R_a}{r^2} \right) f'_1(z, t) + \left(\frac{R_a}{r^2} \right)^2 f'_2(z, t) + \dots \right\} \quad (5)$$

$$v = \left\{ 2 \left(\frac{R_a}{r^2} \right)^2 f_1(z, t) + 4 \left(\frac{R_a}{r^2} \right)^3 f_2(z, t) + \dots \right\} \quad (6)$$

and

$$p = h(z, t) + R_a \times \left\{ h_0(z, t) \ln r + \left(\frac{R_a}{r^2} \right) h_1(z, t) + \left(\frac{R_a}{r^2} \right)^2 h_2(z, t) + \dots \right\}, \quad (7)$$

where the primes denote partial differentiation with respect to z .

The boundary conditions on the functions f_n and their derivatives are

$$\begin{aligned} f'_n(\pm 1, t) &= 0 & n &= 0, 1, 2, \dots \\ f_n(\pm 1, t) &= 0 & n &= 1, 2, \dots \end{aligned} \quad (8)$$

and

$$f_0(1, t) - f_0(-1, t) = 2 \cos \alpha t,$$

which upon choosing

$$f_0(-1, t) = -\cos \alpha t$$

gives

$$f_0(1, t) = \cos \alpha t$$

The expressions for the velocity components (5) and (6) satisfy the continuity equation. Substituting (5), (6) and (7) in (1) and (2), and equating coefficients of equal powers in r , reduces the Navier-Stokes equations to an infinite set of systems of simultaneous linear partial differential equations. The first two systems considered here are:

System I

$$\begin{aligned} \frac{\partial^3 f_0}{\partial z^3} - \frac{\partial^2 f_0}{\partial t \partial z} &= h_0 \\ \frac{\partial h_0}{\partial z} &= 0 \quad \text{i.e., } h_0(z, t) = h_0(t) \end{aligned} \quad (9)$$

The differential equation for h is

$$\frac{\partial h}{\partial z} = 0 \quad \text{i.e., } h(z, t) = h(t), \tag{10}$$

where $h(t)$ is determined from a known pressure at a point in the flow.

System II

$$\frac{\partial^3 f_1}{\partial z^3} - \frac{\partial^2 f_1}{\partial t \partial z} = -2h_1 - \left(\frac{\partial f_0}{\partial z} \right)^2 \tag{11}$$

$$\frac{\partial h_1}{\partial z} = 0 \quad \text{i.e., } h_1(z, t) = h_1(t)$$

b) *Solution of system I*

The solution of (9) subject to the boundary conditions (8) represents the limiting case when $(R_a/r^2) \rightarrow 0$. The linearity of (9) and the form the boundary conditions suggest a solution of the form

$$f_0 = F_0(z) \cos \alpha t + G_0(z) \sin \alpha t \tag{12}$$

and

$$h_0 = H_0 \cos \alpha t + P_0 \sin \alpha t \tag{13}$$

Substitution of (12) and (13) into (9) yields

$$F_0''' - \alpha G_0' = H_0 \tag{14}$$

and

$$G_0''' + \alpha F_0' = P_0 \tag{15}$$

The boundary conditions on F_0 and G_0 and their derivatives are

$$\begin{aligned} F_0(\pm 1) = \pm 1, \quad F_0'(\pm 1) = 0 \quad \text{and} \\ G_0(\pm 1) = G_0'(\pm 1) = 0 \end{aligned} \tag{16}$$

The solutions of (14) and (15) subject to the boundary conditions (16) are

$$\begin{aligned} F_0 = \frac{1}{2\lambda^2} [P_0 z + \lambda\{(B_0 - C_0) \operatorname{sh} \lambda z \cos \lambda z + \\ + (B_0 + C_0) \operatorname{ch} \lambda z \sin \lambda z\}] \end{aligned} \tag{17}$$

and

$$G_0 = \frac{1}{2\lambda^2} [-H_0 z + \lambda\{(B_0 + C_0) \operatorname{sh} \lambda z \cos \lambda z + (C_0 - B_0) \operatorname{ch} \lambda z \sin \lambda z\}] \quad (18)$$

where

$$\lambda = \sqrt{\alpha/2},$$

$$B_0 = \frac{1}{k} [4\lambda^2(-\operatorname{ch} \lambda \cos \lambda) + 2\lambda(\operatorname{sh} \lambda \cos \lambda + \operatorname{ch} \lambda \sin \lambda)]$$

$$C_0 = \frac{1}{k} [4\lambda^2(-\operatorname{sh} \lambda \sin \lambda) + 2\lambda(\operatorname{ch} \lambda \sin \lambda - \operatorname{sh} \lambda \cos \lambda)]$$

$$H_0 = \frac{1}{k} [2\lambda^3(\sin 2\lambda - \operatorname{sh} 2\lambda)] \quad (19)$$

$$P_0 = \frac{1}{k} [4\lambda^4(\operatorname{ch} 2\lambda + \cos 2\lambda) - 2\lambda^3(\operatorname{sh} 2\lambda + \sin 2\lambda)] \quad (20)$$

and

$$k = [2\lambda^2(\operatorname{ch} 2\lambda + \cos 2\lambda) - 2\lambda(\operatorname{sh} 2\lambda + \sin 2\lambda) + (\operatorname{ch} 2\lambda - \cos 2\lambda)]$$

c) Solution of system II

Substituting for $(\partial f_0/\partial z)^2$ from the solution of System I into the right-hand side of (11) will contribute terms with $\cos^2 \alpha t$ and $\sin^2 \alpha t$. These, in turn, can be reduced to terms with $\cos 2\alpha t$, $\sin 2\alpha t$ and steady-state, i.e., time-independent terms. Taking into account these circumstances, one can express the solution for System II, (11), in the form

$$f_1 = F_s(z) + F_1(z) \cos 2\alpha t + G_1(z) \sin 2\alpha t \quad (21)$$

and

$$h_1 = H_s + H_1 \cos 2\alpha t + P_1 \sin 2\alpha t \quad (22)$$

Substituting these expressions into (11), yields

$$F_s''' = -2H_s - \frac{1}{2}(F_0'^2 + G_0'^2) \quad (23)$$

$$F_1''' - 2\alpha G_1' = -2H_1 + \frac{1}{2}(G_0'^2 - F_0'^2) \quad (24)$$

and

$$G_1''' + 2\alpha F_1' = -2P_1 - F_0'G_0' \quad (25)$$

The boundary conditions on F_s, F_1, G_1 and their derivatives are

$$F_s(\pm 1) = F'_s(\pm 1) = 0$$

$$F_1(\pm 1) = F'_1(\pm 1) = 0$$

and

$$G_1(\pm 1) = G'_1(\pm 1) = 0 \tag{26}$$

The solution of (23) subject to the boundary conditions, (26), is

$$F_s = A_s(\frac{1}{3}z^3 - z) + \left(\frac{1}{8\lambda k}\right) [2\lambda z(\text{ch } 2\lambda - \cos 2\lambda) + \\ - (\text{sh } 2\lambda z - \sin 2\lambda z)] + (B_s - C_s) \text{ch } \lambda z \sin \lambda z + \\ - (B_s + C_s) \text{sh } \lambda z \cos \lambda z \tag{27}$$

with

$$H_s = \frac{1}{16} \left[-\frac{(P_0^2 + H_0^2)}{\lambda^4} + \frac{15(\text{sh } 2\lambda - \sin 2\lambda) - 6\lambda(\text{ch } 2\lambda - \cos 2\lambda)}{\lambda k} \right] \tag{28}$$

where

$$A_s = \left(\frac{1}{16\lambda k}\right) [6\lambda(\text{ch } 2\lambda - \cos 2\lambda) - 15(\text{sh } 2\lambda - \sin 2\lambda)]$$

$$B_s = -\left(\frac{1}{2\lambda k^2}\right) [2\lambda^2(-\text{ch } 3\lambda \cos \lambda - \text{ch } \lambda \cos 3\lambda - 2 \text{ch } \lambda \cos \lambda) + \\ + 2\lambda(\text{sh } 3\lambda \cos \lambda + \text{ch } \lambda \sin 3\lambda + \text{sh } \lambda \cos \lambda + \text{ch } \lambda \sin \lambda) + \\ + (-\text{ch } 3\lambda \cos \lambda + \text{ch } \lambda \cos 3\lambda)]$$

and

$$C_s \text{ch } \lambda \cos \lambda = B_s \text{sh } \lambda \sin \lambda$$

The solutions of (24) and (25) subject to the boundary conditions, (26), constitute the fluctuating components of System II. The detailed expressions for F_1, G_1, H_1 , and P_1 are long and are omitted to conserve space; readers interested in these expressions are invited to write to the author.

§ 3. Results and discussions

a) *Velocity distribution*

We define a dimensionless radial velocity such that

$$w^* = \frac{wr}{R_a}$$

Substituting for f_0 and f_1 from (12) and (21) into (5), and neglecting higher order terms, yields

$$\begin{aligned} w^* &= f'_0 + R_a^* f'_1 \\ &= (F'_0 \cos \alpha t + G'_0 \sin \alpha t) + R_a^* (F'_s + F'_1 \cos 2\alpha t + G'_1 \sin 2\alpha t) \end{aligned} \quad (29)$$

The first term on the right-hand side of (29) represents the radial velocity for $R_a^* = 0$, i.e. as $r \rightarrow \infty$, while the second term represents the effect of the nonlinear inertia. The nonlinear-inertia contribution is in the form of steady streaming, F'_s , superimposed on an oscillating motion of frequency twice that of the source strength.

Profiles for the amplitude of the first-harmonic fluctuation, $(f'_0)_a$, are presented in Fig. 2. From Fig. 2 it is shown that $(f'_0)_a$ approaches a parabolic distribution as $\alpha \rightarrow 0$; while for high frequencies it assumes a fairly uniform value across the central portion of the flow domain and reaches its maximum values close to the solid boundaries.

The distributions of the steady perturbation term, F'_s for various values of α are shown in Fig. 3. From Fig. 3 it is shown that F'_s is small when compared with $(f'_0)_a$. Also, calculations of the amplitude of the second-harmonic fluctuation have shown that it is of the same order as F'_s and that their combined contribution to the velocity distribution can be neglected for high values of α .

The instantaneous radial velocity distributions for $\alpha = 100$ and for $R_a^* = 0$ and $R_a^* = 3.00$ are shown in Fig. 4. The magnitudes of the nonlinear inertia contributions to the velocity distributions are very small to be shown in these graphs. The velocity distributions presented in Fig. 4 show that the flow exhibits a boundary-layer character in the neighbourhood of the solid boundary, and that the flow in the central region lags behind that in layers near the boundaries.

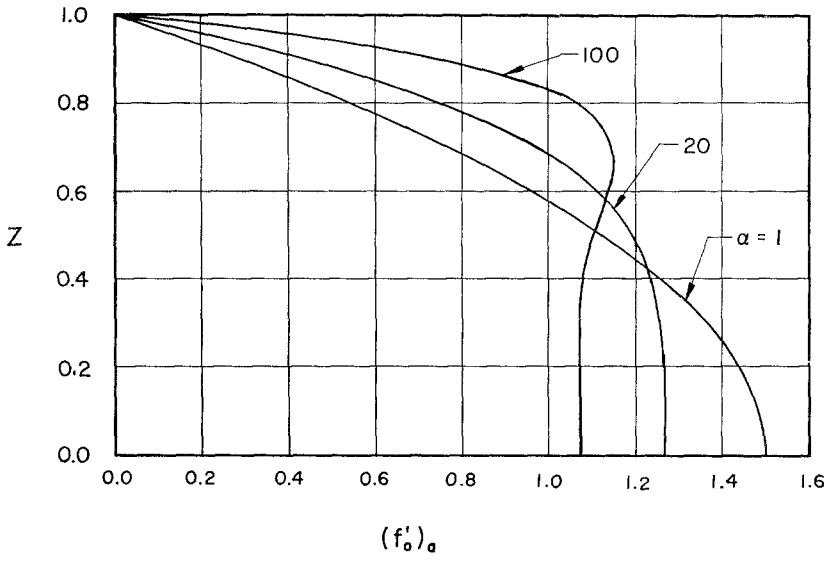


Fig. 2. Amplitude of f'_0 , $(f'_0)_a$.

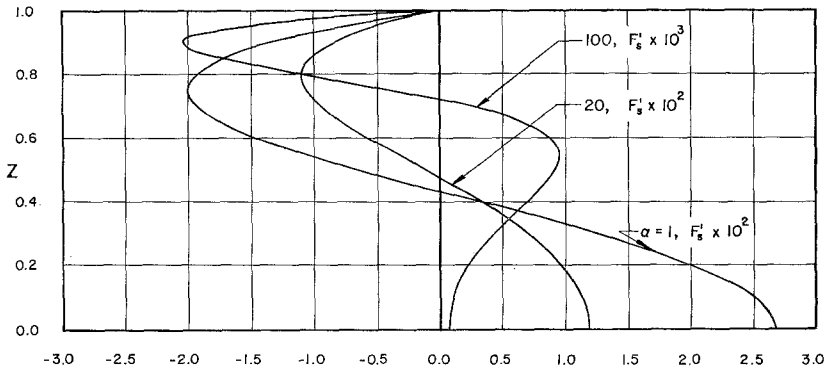


Fig. 3. Steady radial velocity, F'_s .

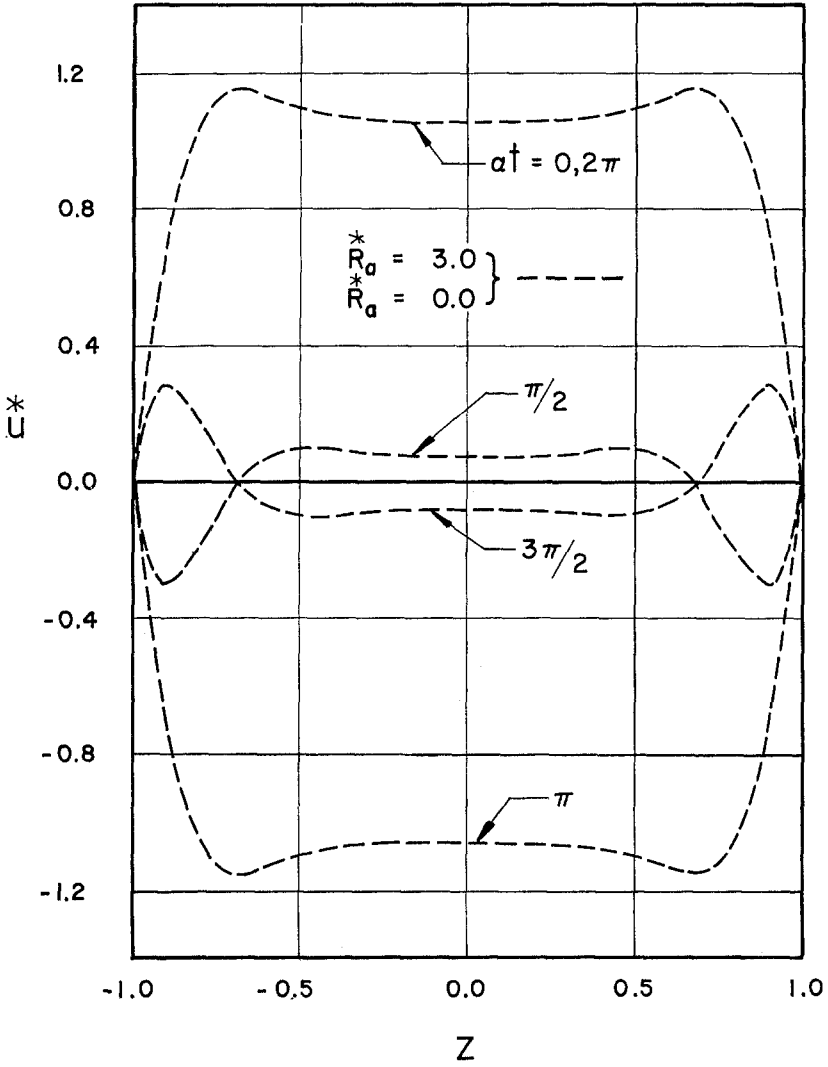


Fig. 4. Radial velocity distributions for $\alpha = 100$, $R_a^* = 3.0$ and $R_a^* = 0$.

b) *Pressure distribution*

Neglecting terms of higher order than R_a^* , and using (10), the pressure distribution is of the form

$$p = h(t) + R_a[h_0(t) \ln r + h_1(t)R_a^*]$$

where $h(t)$ is a function of time only and is determined from a known pressure at some cross-section in the flow. Assuming that the pressure is known at $r = R$, and using (13) and (22), the ex-

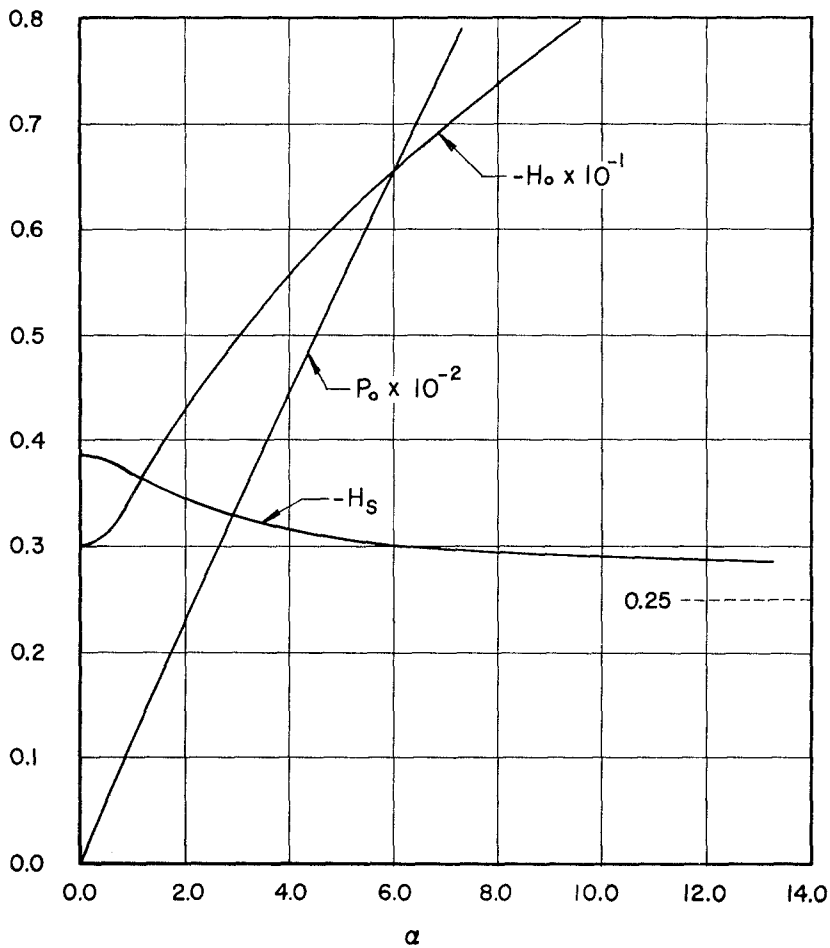


Fig. 5. Variation of H_0 , P_0 , and H_s with α .

pression for the pressure distribution is

$$\begin{aligned}
 \dot{p}^* &= \frac{p(r, t) - p(R, t)}{R_a} \\
 &= \left[(H_0 \cos \alpha t + P_0 \sin \alpha t) \ln \left(\frac{r}{R} \right) + (H_s + H_1 \cos 2\alpha t + \right. \\
 &\quad \left. + P_1 \sin 2\alpha t) \left(\frac{R_a}{r^2} \right) \left(1 - \frac{r^2}{R^2} \right) \right] \quad (30)
 \end{aligned}$$

Values of the pressure coefficients for various α are given in Table I, and are presented graphically in Figs. 5 and 6. From Table I it is shown that H_s and H_1 are of the same order.

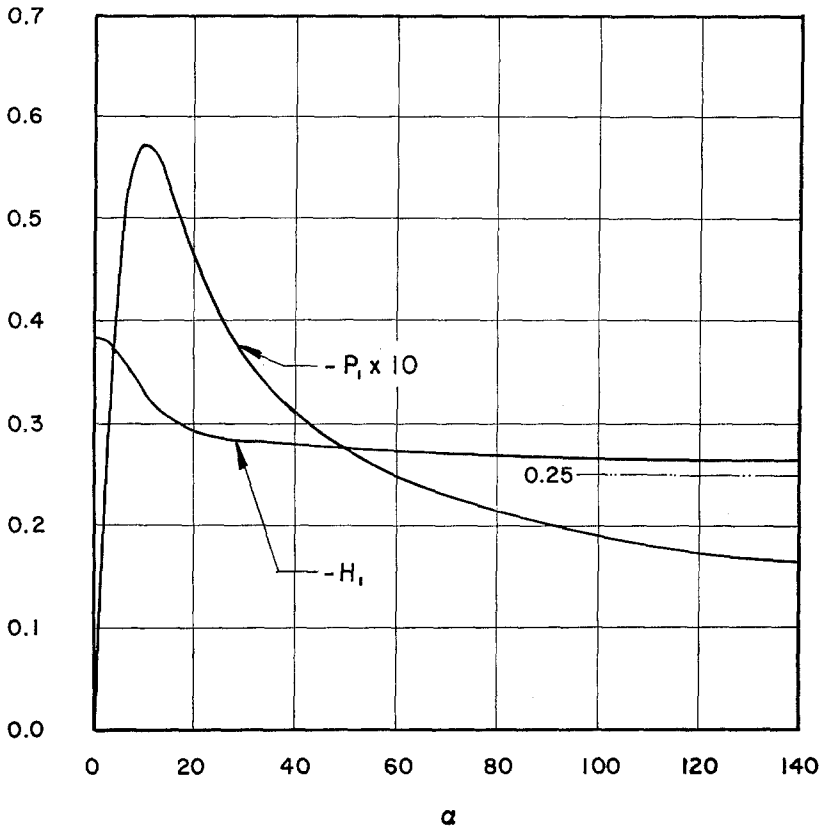


Fig. 6. Variation of H_1 and P_1 with α .

TABLE I

α	1	10	20	30	40	50
$-H_0(10^{-1})$	0.3006	0.3473	0.4289	0.4993	0.5582	0.6098
$P_0(10^{-2})$	0.0120	0.1179	0.2294	0.3371	0.4433	0.5488
$-H_s$	0.3855	0.3701	0.3456	0.3283	0.3171	0.3095
$-H_1$	0.3846	0.3286	0.2953	0.2848	0.2798	0.2765
$-P_1(10)$	0.1132	0.5737	0.4608	0.3639	0.3095	0.2749

α	100	200	300	400	500	600
$-H_0(10^{-1})$	0.8141	1.1050	1.3288	1.5177	1.6843	1.8349
$P_0(10^{-2})$	1.0699	2.0994	3.1220	4.1410	5.1578	6.1729
$-H_s$	0.2906	0.2778	0.2723	0.2691	0.2670	0.2654
$-H_1$	0.2685	0.2630	0.2606	0.2592	0.2582	0.2575
$-P_1(10)$	0.1916	0.1339	0.1087	0.0938	0.0837	0.0763

Pressure coefficients

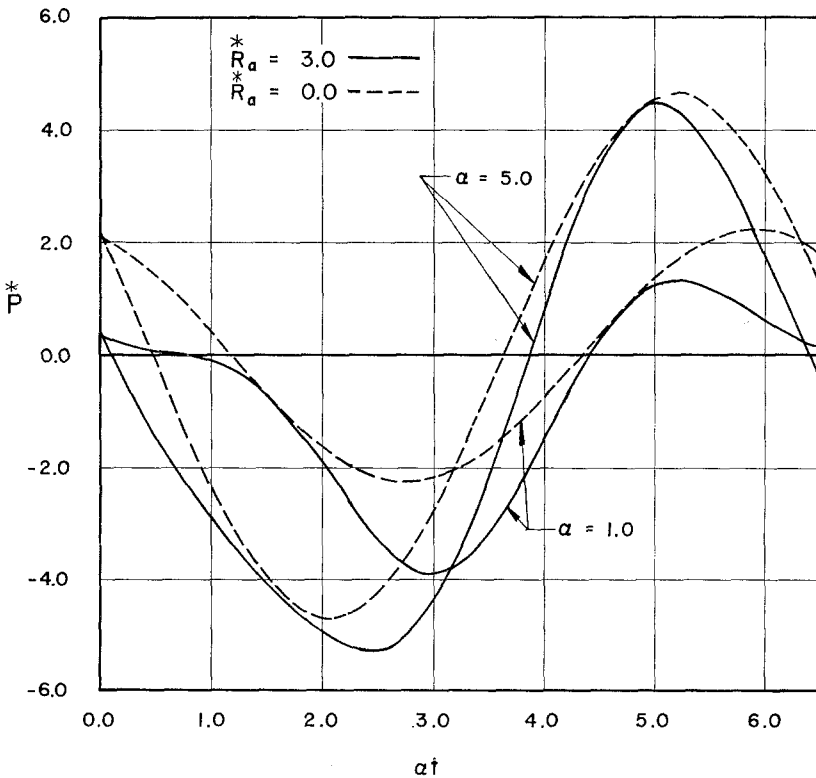


Fig. 7. Variation of p^* with time for small α , $\nu/R = 0.5$.

Examination of the expressions for the pressure coefficients shows that $H_0/\lambda \rightarrow -1$, $P_0/\alpha \rightarrow 1$, $H_s \rightarrow -\frac{1}{4}$, $H_1 \rightarrow -\frac{1}{4}$, and $P_1 \rightarrow 0$ as $\alpha \rightarrow \infty$.

The variation of p^* with time for $r/R = 0.5$, $R_a^* = 0$ and $R_a^* = 3.0$, and for various α are presented in Figs. 7 and 8. From Figs. 7 and 8 it is shown that the effect of the nonlinear-inertia is significant for small frequencies, while for large frequencies the effect is negligible. For $R_a^* = 0$, the pressure oscillates with the same frequency as the source strength and with a phase lead that approaches $\pi/2$ as α approaches ∞ .

The quasi-steady state pressure distribution, valid in the limit as $\alpha \rightarrow 0$, agrees with the results of ref. [2] and is given by

$$p^* = \cos \alpha t \left[-3 \ln \left(\frac{r}{R} \right) - \frac{27R^*}{35} \left(1 - \frac{r^2}{R^2} \right) \right], \quad (31)$$

where $R^* = R_a^* \cos \alpha t$.

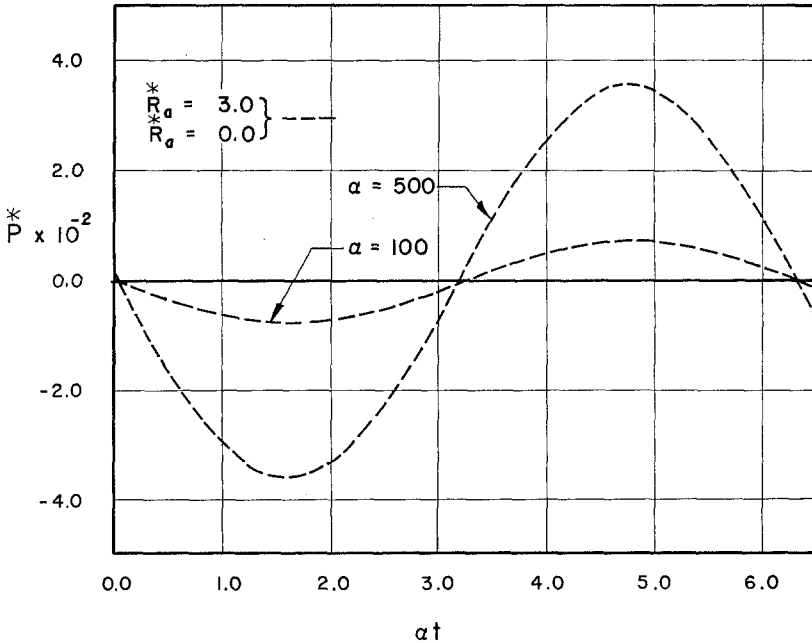


Fig. 8. Variation of p^* with time for large α , $r/R = 0.5$.

Substituting the asymptotic expressions for P_0 and H_0 in (30), one obtains

$$p^* \rightarrow \alpha \cos\left(\alpha t + \frac{\pi}{2}\right) \ln\left(\frac{R}{r}\right) \quad \text{as } \alpha \rightarrow \infty \quad (32)$$

c) *Skin friction*

The shear stress at the upper boundary is given by

$$\begin{aligned} \bar{\tau}_1 &= -\mu \left(\frac{\partial \bar{u}}{\partial z}\right)_{z=a} = -\frac{\rho v^2}{a^2} \left(\frac{\partial u}{\partial z}\right)_{z=1} \\ &= -\frac{\mu Q_0}{4\pi a^2 \bar{r}} [f_0''(1, t) + R_a^* f_1(1, t)] \end{aligned}$$

Defining a dimensionless shear stress as $\tau_1 = \bar{\tau}_1 / (\mu Q_0 / 4\pi a^2 \bar{r})$, we have

$$\begin{aligned} \tau_1 &= -\{[F_0''(1) \cos \alpha t + G_0''(1) \sin \alpha t] + \\ &\quad + R_a^* [F_s''(1) + F_1'(1) \cos 2\alpha t + G_1'(1) \sin 2\alpha t]\} \quad (33) \end{aligned}$$

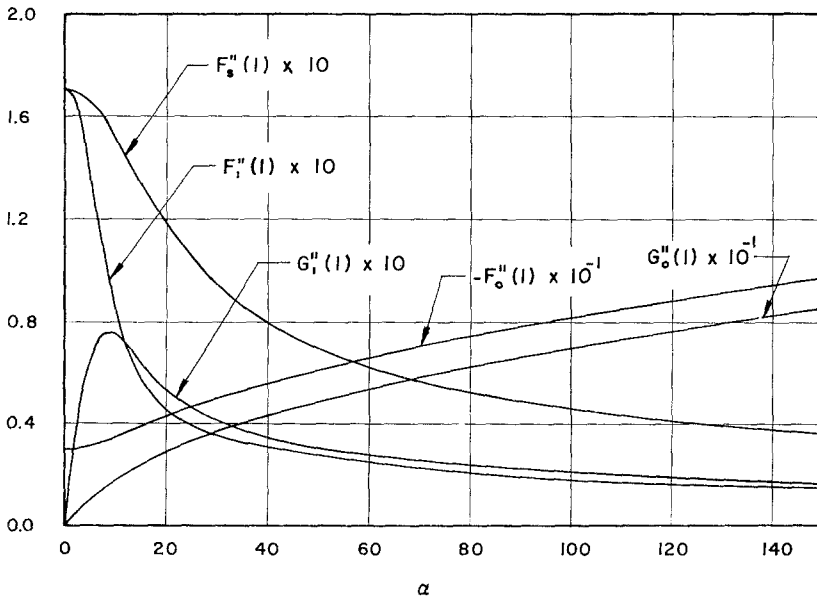


Fig. 9. Shear stress coefficients.

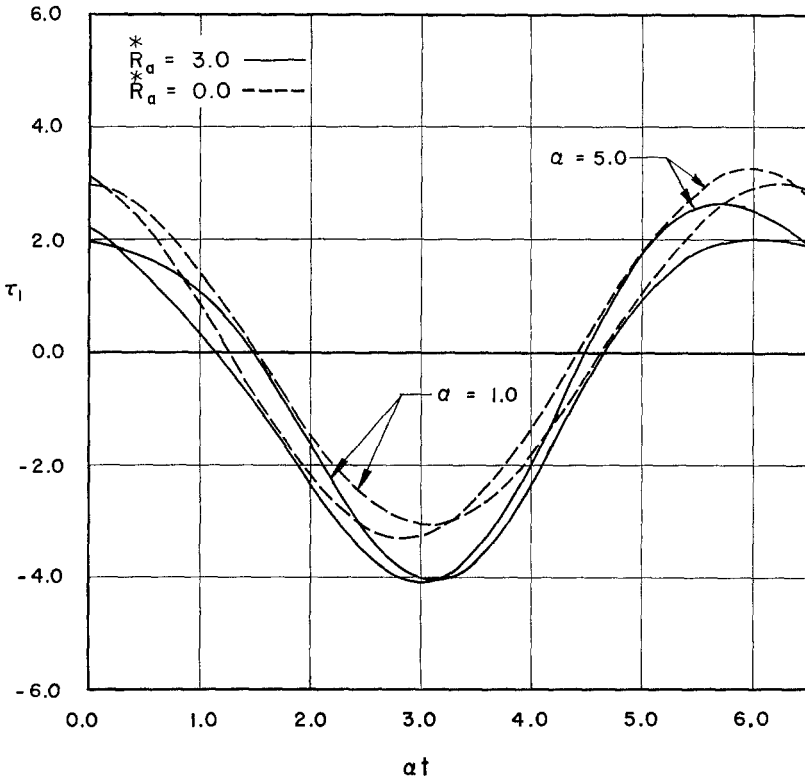


Fig. 10. Variation of τ_1 with time for small α .

The shear stress coefficients $F_0''(1)$, $G_0''(1)$, $F_s''(1)$, $F_1'(1)$, and $G_1'(1)$ are presented graphically in Fig. 9. Examination of the expressions for the shear stress coefficients shows that $F_0''(1)/\lambda \rightarrow -1$, $G_0''(1)/\lambda \rightarrow 1$, $F_s''(1) \rightarrow 0$, $F_1'(1) \rightarrow 0$, and $G_1'(1) \rightarrow 0$ as $\alpha \rightarrow \infty$.

The variation of τ_1 with time for $R_a^* = 0$ and $R_a^* = 3$, and for various values of α are presented in Figs. 10 and 11. Fig. 10 indicates that the effect of the nonlinear-inertia can be significant for small α , while Fig. 11 shows that such an effect can be negligible for high values of α . As $\alpha \rightarrow 0$ the shear stress approaches values obtained from the quasi-steady-state solution, given by the expression

$$\tau_1 = \cos \alpha t \left(3 - \frac{12}{35} R^* \right) \quad (34)$$

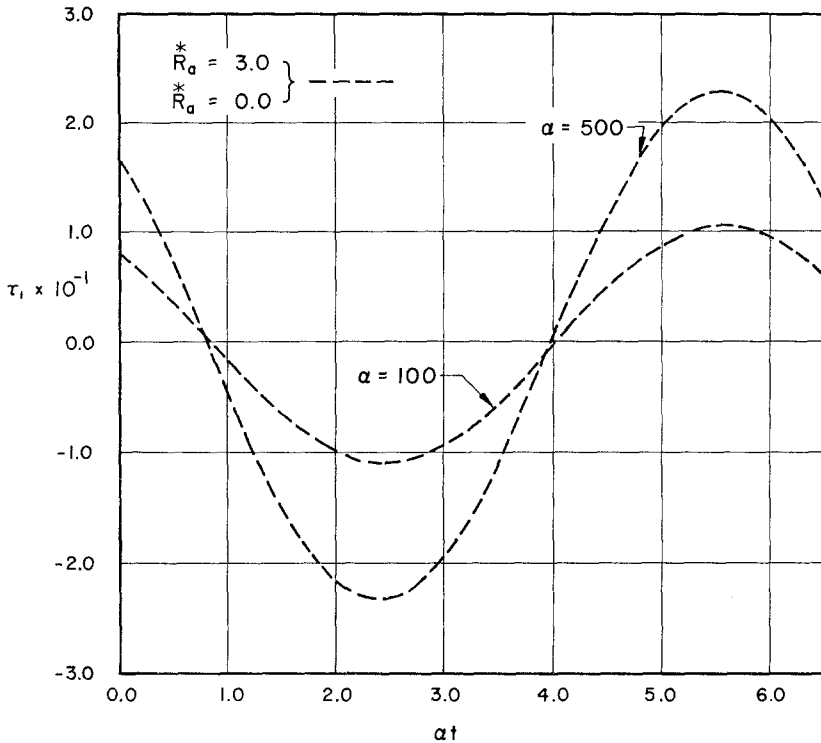


Fig. 11. Variation of τ_1 with time for large α .

For $R_a^* = 0$ the shear stress at the boundary oscillates with the same frequency as the source strength, and with a phase lead that approaches $\pi/4$ as α approaches ∞ , Fig. 11.

Substituting the asymptotic values of the shear stress coefficients into (33), we obtain

$$\tau_1 \rightarrow \sqrt{2} \lambda \cos\left(\alpha t + \frac{\pi}{4}\right), \text{ as } \alpha \rightarrow \infty \tag{35}$$

Received 29 October 1974

REFERENCES

- [1] UCHIDA, S., ZAMP 7 (1956) 403.
- [2] NA, T. Y., E. G. NIELSEN and J. D. GROSSMAN, ASME publication 67 - WA/FE - 20, Winter Annual Meeting, Nov. 1967.
- [3] ELKOUH, A. F., Appl. Sci. Res. 21 (1969) 284.